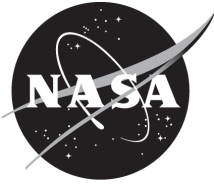# Electron Beam Welding of Pure Tungsten Hex Cans for Nuclear Thermal Propulsion Engines

Z.S. Courtright and K.M. Benensky
Marshall Space Flight Center, Huntsville, Alabama

The NASA STI Program…in Profile

Since its founding, NASA has been dedicated to the advancement of aeronautics and space science. The NASA Scientific and Technical Information (STI) Program Office plays a key part in helping NASA maintain this important role.

The NASA STI Program Office is operated by Langley Research Center, the lead center for NASA's scientific and technical information. The NASA STI Program Office provides access to the NASA STI Database, the largest collection of aeronautical and space science STI in the world. The Program Office is also NASA's institutional mechanism for disseminating the results of its research and development activities. These results are published by NASA in the NASA STI Report Series, which includes the following report types:

- TECHNICAL PUBLICATION. Reports of completed research or a major significant phase of research that present the results of NASA programs and include extensive data or theoretical analysis. Includes compilations of significant scientific and technical data and information deemed to be of continuing reference value. NASA's counterpart of peer-reviewed formal professional papers but has less stringent limitations on manuscript length and extent of graphic presentations.

- TECHNICAL MEMORANDUM. Scientific and technical findings that are preliminary or of specialized interest, e.g., quick release reports, working papers, and bibliographies that contain minimal annotation. Does not contain extensive analysis.

- CONTRACTOR REPORT. Scientific and technical findings by NASA-sponsored contractors and grantees.

- CONFERENCE PUBLICATION. Collected papers from scientific and technical conferences, symposia, seminars, or other meetings sponsored or cosponsored by NASA.

- SPECIAL PUBLICATION. Scientific, technical, or historical information from NASA programs, projects, and mission, often concerned with subjects having substantial public interest.

- TECHNICAL TRANSLATION. English-language translations of foreign scientific and technical material pertinent to NASA's mission.

Specialized services that complement the STI Program Office's diverse offerings include creating custom thesauri, building customized databases, organizing and publishing research results…even providing videos.

For more information about the NASA STI Program Office, see the following:

- Access the NASA STI program home page at <http://www.sti.nasa.gov>

- E-mail your question via the Internet to <help@sti.nasa.gov>

- Phone the NASA STI Help Desk at 757–864–9658

- Write to:
  NASA STI Information Desk
  Mail Stop 148
  NASA Langley Research Center
  Hampton, VA 23681–2199, USA

Electron Beam Welding of Pure Tungsten Hex Cans for Nuclear Thermal Propulsion Engines

Z.S. Courtright and K.M. Benensky
Marshall Space Flight Center, Huntsville, Alabama

Acknowledgments

TABLE OF CONTENTS

LIST OF FIGURES

LIST OF TABLES

LIST OF ABBREVIATIONS AND ACRONYMS

cermet   ceramic metal

DBTT   ductile to brittle transition temperature

EBW   electron beam welding/welds

FC   focus current

HAZ   heat-affected zone

IPM   inches per minute

MSFC   Marshall Space Flight Center

NTP   nuclear thermal propulsion

PWHT   post-weld heat treat(ment)/treated

TECHNICAL MEMORANDUM

**ELECTRON BEAM WELDING OF PURE TUNGSTEN HEX CANS
FOR NUCLEAR THERMAL PROPULSION ENGINES**

1. INTRODUCTION

Nuclear thermal propulsion (NTP) is an in-space propulsion method currently being developed at the NASA Marshall Space Flight Center (MSFC). NTP systems are a high specific impulse (750–1,100 s), high thrust (15,000–250,000 lb_f) method of propulsion which have the potential to allow for faster transit times when optimizing for high ΔV. In the nuclear rocket engine, the heat from the nuclear fission reaction is transferred to a low molecular mass propellant (such as hydrogen). Hot propellant is expanded through a nozzle to generate thrust.

Development of ceramic metal (cermet) fuel systems for NTP applications is currently ongoing at MSFC. In cermet fuel systems, ceramic fissile fuel particles such as uranium nitride or uranium dioxide are dispersed within a net-shaped, high-density structural matrix. The composite material is cladded by a protective metal structure to make up an NTP fuel element. Cladding materials must be able to withstand the demanding operating conditions required of the engine as well as retain a hermetic seal to allow for retention of fuel element structural integrity, prevent hydrogen attack or migration of the ceramic fuel, and limit release of fission products during operation. For NTP applications, tungsten is a prime material for both the metal matrix and cladding in cermet fuel systems because of its high melting point, high temperature strength, and compatibility with hot hydrogen. If a weld in tungsten with the capability of holding a hermetic seal is achievable, tungsten becomes a strong candidate for NTP applications.[1,2] This Technical Memorandum focuses on determining the weldability of pure tungsten using electron beam welding (EBW).

Tungsten appears well suited for NTP applications, but it has a high ductile to brittle transition temperature (DBTT) dependent upon chemical composition, structure/stress distribution, and mechanical conditions.[3–6] Therefore, it is highly subject to brittle fracture. Because of its high susceptibility to brittle fracture, it is very difficult to weld.

EBW was chosen for joining pure tungsten because of its low heat input compared to gas tungsten arc welding. Reduced heat input can be directly correlated with an increase in ductility of a tungsten weld.[3,5,7] EBW is a high energy density welding process in which a stream of electrons penetrates a weld joint in a deep, narrow spike in contrast to a broad gas tungsten arc weld pool.[8]

The investigation initially focused on EBW of tungsten plates of both 0.01 in and 0.03 in thickness to determine if EBW could weld pure tungsten without the presence of visual defects—particularly cracking—in the welds. Variation in the weld procedure and post-weld heat treatment (PWHT) was used to improve the surface appearance of flat EBWs on a pure tungsten sheet.

The investigation moved on to weld 0.05-in-thick hexagonal tungsten cans with a weld joint thickness of 0.025 in. The goal for welding the pure tungsten hex cans was to avoid any visual surface defects and generate a weld capable of a hermetic seal. This proved difficult. Cold welds commonly exhibited porosity that leaked air. Hot welds exhibited cracks, typically observed immediately after welding.

Later welds were preheated to increase ductility and decrease the likelihood of through-thickness cracking. PWHT was used to arrest microcrack growth both in the flat weld samples and hexagonal weld samples.

2. PROCEDURE

2.1 Part 1: Electron Beam Welding Pure Tungsten Plates

Thin tungsten plates of 0.03 in and 0.01 in thickness were machined into 3 in by 3 in squares to utilize the material efficiently. The plates were butt welded together with varying parameters until optimal weld parameters were determined. The parameters were considered optimal if they produced a visibly defect-free weld; i.e., no cracking or porosity. One parameter set was determined for the 0.01 and 0.03 in configurations.

Four welds were made at each thickness using the optimized parameters.. Two of the four welds were PWHT at 1037.78 °C and the other two were observed in the as-welded condition. Both the as-welded and PWHT samples were visually inspected after sitting for 24 hours after welding. The weld quality was initially determined by the presence of cracking in an as-welded sample, which indicated a poor weld. The PWHT welds were also inspected after PWHT to determine if any crack growth occurred during stress relief.

All four welds for the two thicknesses were cut into macro samples for microstructural and macroscopic inspection. The knowledge gained from this initial study was used in the follow-on study focusing on welding pure tungsten hex cans.

2.2 Part 2: Electron Beam Welding Pure Tungsten Hex Cans

The hex can samples were initially machined into 1-in-tall hexagons. A counterbore was machined into one end of each hexagon to a depth of 0.025 in so the hex cap would have a snug fit in the hexagon. The hex cap was machined from 0.03-in-thick plate and then final machined to a thickness of 0.025 in so the top of the hex can would have a flat joint interface along the inner edge of the hexagon. Each set of hex cans and caps were labeled to indicate which number each sample was in the weld experiment. The order of the samples was based on the quality of the machining. The first sample reflected the lowest quality machining and the last sample reflected the highest quality machining based on exfoliation caused by the brittle nature of pure tungsten.

Following machining and labeling of each hex can assembly, each sample was wiped with acetone just prior to being set up in the EBW fixture. Each of the nine weld samples was welded with EBW in the setup shown in figure 1. The beginning samples used parameters similar to those developed with the flat plate welds. Those parameters were quickly established as inadequate, due to holes and cracks observed with visual inspection, so parameter development continued throughout all nine samples. Each sample had a variation in parameters compared to the last sample. This meant the experiment could only focus on parameter development rather than repeatability of an EBW.
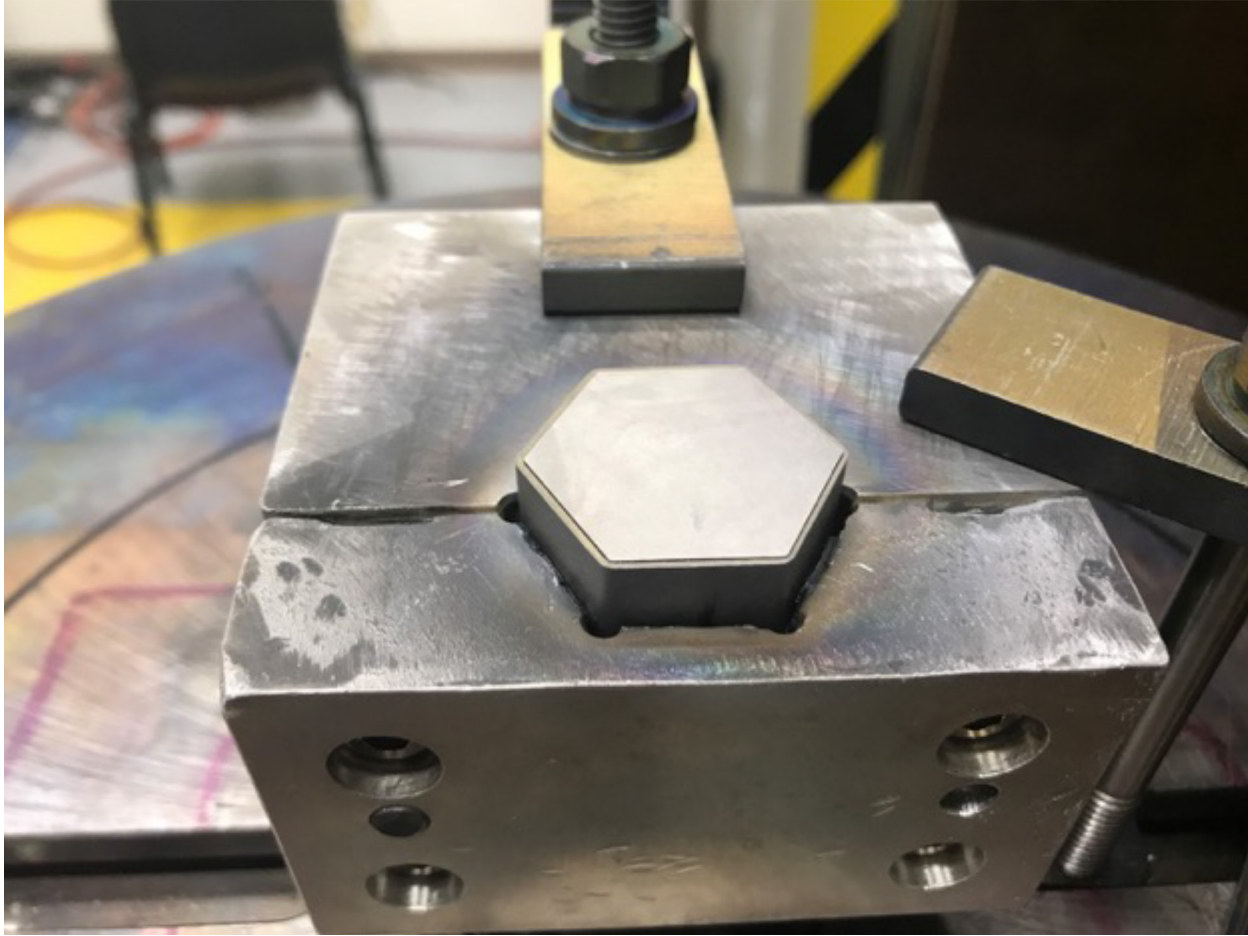
Figure 1. Image of EBW_Hex8 assembled in the EBW fixture prior to welding.

Once a weld was made along the top edge of a hex can assembly and the welding engineer decided to pull the sample from the electron beam welder, the weld sample was immediately put into an insulating material within a cardboard box to decrease cooling rates and, therefore, help to distribute residual stresses.[8] The last five weld samples had hot copper pieces put just outside the insulating material to better ensure uniform cooling of the samples.

The 'insulator box' was then transported by the welding engineer to an induction furnace for PWHT at 1400 °C, shown in figure 2. The induction furnace was then opened and the sample was inserted into the center of the furnace prior to following the furnace startup procedures to complete the PWHT.[4] This PWHT lasted for up to 6 hours.

Figure 2. Oven used for PWHT of all pure tungsten hex cans.

The following business day the sample was removed from the induction furnace and pre-pared for pressure testing. To prepare for pressure testing, an aluminum insert was made to fit into the open end of the hex can. This aluminum insert had a barbed fitting on one end that could easily be inserted into an air hose attached to a regulator. The regulator setup is shown in figure 3 and the aluminum insert, attached to EBW_Hex8, is shown in figure 4. Multiple methods were used to ensure that the fitting and hex can had an airtight fit-up. Initial pressure tests used teflon tape and electrical tape to attempt to create an airtight fit-up. This technique was not satisfactory. Instead, a low melting point polymer was applied to the insert/hex can interface by heating the polymer with a heat gun and spreading it across the interface. Once the polymer cooled, the sample was ready for pressure testing. Pressure testing was done by using air pressure on the inside of the weld joint while the outside of the weld joint was submerged in water.

Figure 3. Regulator setup for pressure testing of the pure tungsten hex cans.

Figure 4. Pressure test setup with EBW_Hex8 attached to the pressure hose and aluminum hex fitting.

It was found that the pressure regulator only became accurate above 5 psi. Therefore, all pressures held under 5 psi were subject to debate and weld parameters had to be repeated to ensure proof of a hermetic seal. The initial pressure testing was done by slowly opening the regulator valve to allow up to 5 psi of pressure to impinge upon the weld root. It was recorded if no bubbles were seen at this point. Then the regulator was opened to a point where 10 psi and then 20 psi was impinging upon the weld root. The formation of bubbles and the location that they came from within the sample was then recorded.

3. RESULTS

The initial study for this experiment focused on EBW of thin, pure tungsten plates. The thickness of the plates was either 0.01 or 0.03 in and the majority of the experiment focused on EBW parameter development. Once the parameters were optimized, the welds were repeated four times for each thickness. Two of the four optimized welds for each thickness were PWHT at 1037.78 °C. This temperature was chosen because it was the highest temperature possible for the furnace used; therefore, it was as close to the desired temperature of 1400 °C as possible for the furnace. The 1400 °C temperature was used in another experiment which focused on the weldability of pure tungsten and it was found to marginally improve ductility.[7]

As evidenced by figure 5, both the 0.01- and 0.03-in-thick tungsten plates exhibited cracking when no PWHT was used. The cracking was much more evident in the thinner of the plates as shown in figure 5(a).
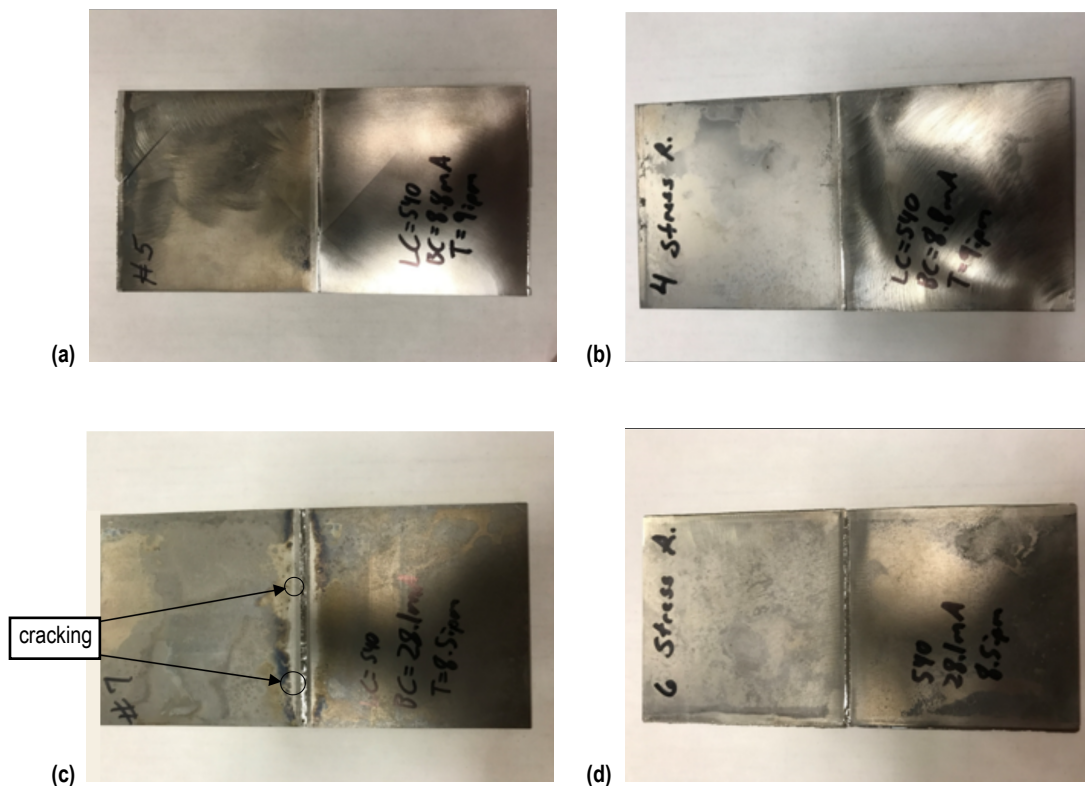

Figure 5. Images of electron beam butt welds on thin, pure tungsten plates: (a) 0.01-in tungsten with no PWHT, (b) 0.01-in tungsten with PWHT, (c) 0.03-in tungsten with no PWHT, and (d) 0.03-in tungsten with PWHT.

The results of the study using EBW to butt weld pure tungsten plates were then carried forward for a study of EBW of tungsten hex cans for potential nuclear thermal applications. For the hex can study, only nine sample assemblies were available because of a lack of available material in hexagonal form and the high expense associated with machining pure tungsten for the complex geometry necessary for the experiment. The first two of the nine samples were used primarily for initial parameter development and the first sample was used for testing of the induction furnace. The induction furnace was used to achieve the desired heat treatment temperature of 1400 °C. Samples 3 through 9 were used to optimize parameters to eliminate any surface porosity or cracking. It was found that surface porosity was more likely with lower heat input welds. Furthermore, when heat input was too high, the welds tended to crack during cooling, or soon after, due to the buildup of residual stresses. Therefore, it was necessary to balance heat input in an attempt to avoid porosity and cracking. Prior to beginning welding of the hex cans, the can assemblies were visually inspected and the samples with the greatest number of machining defects were labeled first while the near, immaculately machined samples were labeled later. This resulted in welding the less-than-perfect samples first during the parameter development portion of the experiment.

EBW_Hex1, shown in figure 6(a), was made using a hex can with a machining defect along the joint interface. The defect was small and located on one of the corners of the hexagon. Issues with the weld path program led to a need to run the preheat pass three times to ensure that the path would run evenly across the weld joint interface. The heat input of the weld was too high and resulted in burn-through which is easily observed in the side wall of the hex can shown in figure 6(a). The holes were located both on the straight portions and on the corners of the hexagonal weld joint, indicating that the machining defect on the joint interface on the hex can was not the only portion of the weld interface subject to burn-through. The holes were all located on the side wall rather than on top of the hex can, which may have been caused by excessive focus of the electron beam on the outer edge of the weld joint or due to the fact that the hexagon was made from plasma-sprayed tungsten and the hex cap was made from a solid tungsten sheet. Although holes were present, a PWHT was still performed to ensure that the PWHT cycle was correct. PWHT was done in a hydrogen atmosphere after the furnace chamber was purged with argon to reduce oxygen levels to prevent oxidation. After the PWHT, a visual inspection was performed and found no evidence of cracking. This indicated that residual stresses were relieved evenly during the PWHT so brittle fracture did not occur.

Figure 6. Images of all nine pure tungsten hex can samples: (a) EBW_Hex1, (b) EBW_Hex2, (c) EBW_Hex3, (d) EBW_Hex4, (e) EBW_Hex5, (f) EBW_Hex6, (g) EBW_Hex7, (h) EBW_Hex8, and (i) EBW_Hex9.

The initial weld pass for EBW_Hex2, shown in figure 6(b), was too hot and resulted in immediate burn-through causing an emergency stop in the weld after 1 s. After this, another six attempts were made to seal the hole, none of which were successful. The second attempt used a lower beam current than the first and was aborted halfway through the weld cycle because it generated a large amount of surface porosity. The third attempt used a much lower beam current than the first attempt and a higher focus current which helped to partially defocus the beam. This attempt went along the full weld path and the heat input was too low to fully melt the weld joint. The fourth attempt used a beam current 1 mA higher than the third attempt and improved surface appearance in the entire weld aside from the initial burn-through. Attempts five and six also improved surface appearance and attempt seven closed all surface porosity but was unsuccessful in closing the burn-through. No PWHT was done for this sample because it exhibited a large burn-through hole, thus inhibiting it from holding pressure. Cracks propagating from the hole and one of the corners of the weld became visible after the sixth weld attempt and were likely due to excessive heat input causing a thermal gradient which led to high residual stresses along the corners of the weld and along the burn-through defect. These cracks grew and others, which were not observed during visual inspection, appeared over the course of a week and may be attributed to the lack of PWHT. An example of this is shown in the images on the bottom of figure 6(b). The image on the left was taken immediately after welding and the crack was present but had not propagated well into the side wall. The image on the right is a magnification of the overall image and was taken days after welding had been completed. This image showed greater propagation of the crack into the sidewall. Visual inspection 1 week after welding showed many more cracks and greater crack lengths than visual inspection immediately after welding. Photographic images were not optimal for showing the length, number, and size of cracks.

The weld parameters developed from the final weld pass in EBW_Hex2 were used to weld EBW_Hex3. EBW_Hex3, shown in figure 6(c), used a preheat pass, weld pass, and cosmetic pass. The cosmetic pass used the same parameters as the weld pass. After the weld, no holes or cracks were visible so a PWHT was performed. After the PWHT, a pressure test was performed using the pressure test setup shown in figure 4. As soon as the pressure was raised above 0 psi, bubbles began to release from the surface of the weld joint. The bubbles came from one weld defect along the weld path that was located on one of the sides rather than on one of the corners of the hex can. This defect location is indicated with a blue arrow in figure 6(c), and appears to be surface porosity caused by a low weld heat input.

EBW_Hex4, shown in figure 6(d), was made with a slightly hotter weld pass than EBW_Hex3. After welding, the surface had some minor spatter and a few divots were located in the weld. Then, a PWHT was performed prior to pressure testing. One of the divots, located on one of the corners, leaked during pressure testing. This divot is identified by a blue arrow with a star next to it in figure 6(d). Then, as the pressure was increased to 10 psi, two more leaks appeared, both of which also came from corners. These two leaks are identified in figure 6(d) by the two blue arrows with no star next to them. The two worst leaks came from the corners where surface divots existed and became worse due to the propagation of cracks upon pressure testing. (Prior to pressure testing, no cracks were evident.)

Similar to EBW_Hex2, the initial parameters used for EBW_Hex5 resulted in immediate burn-through at the beginning of the weld. This sample, shown in figure 6(e), was then used as a test sample to see if high heat input could seal the hole. Each attempt to seal the hole was run at a higher heat input than the previous attempt. After eight unsuccessful attempts, a preheat pass was run to redistribute the thermal stresses from the previous passes. Next, an attempt was made to fill the hole with a small piece of tungsten and another weld pass was run with a beam current of 23 mA. The small tungsten piece was melted in place but did not fully seal the hole. The heat from the repeated cosmetic passes greater than 24 mA led to significant sidewall cracking (propagating from the large hole and the corners of the hex can). The formation of these holes and cracks led to a reassessment of the welding procedure. It was then decided that a rotating beam pattern may help distribute heat evenly, resulting in a better weld appearance. The rotating beam pattern parameters, used on EBW_Hex6, were used on all of the remaining weld samples. No PWHT was done on this weld because the through-hole was not fully filled and extensive cracking was present.

EBW_Hex6, shown in figure 6(f), used the new beam parameters of beam pattern 5, frequency of 20, x amplitude of 5, y amplitude of 5, and rotation of 5. This weld incorporated, in chronological order, a preheat run, a hot preweld pass, a weld pass, a rerun at the preheat parameters, a cosmetic pass, and finally another pass with the preheat parameters. The use of a preheat pass between the weld pass and cosmetic pass and after the full weld sequence was to avoid the formation of high residual stresses and prevent cracking during the weld sequence. The preweld pass, first used in this weld sample, was added to slightly melt the weld joint so heat distribution during the weld pass would be more uniform. This was also added to potentially increase the ductility of the weld to prevent cracking.[7] During PWHT, the lack of a visible hydrogen flame in the burn stack of the induction furnace caused the welding engineer to decide to use argon as the inert atmosphere in the furnace rather than hydrogen. This is believed to have no effect on weld stress relief.

The pressure test of EBW_Hex6 yielded promising results because upon initial pressurization, between 0 and 5 psi, no bubbles were evident along the weld joint. Upon further pressurization to 20 psi, bubbles began to release from the weld joint at a rate of about one per second. The location in which the bubbles appeared are denoted by a blue arrow in figure 6(f). The pressure test results indicated that, at very low pressures, a hermetic seal was present and further testing is necessary to determine repeatability at the parameters used for this weld. This weld had no visual cracking but did have visual surface pores so the next weld sample used different parameters in an attempt to create a visually defect-free weld.

EBW_Hex7, shown in figure 6(g), used a preweld pass to increase ductility like EBW_Hex6. This resulted in a more uniform weld but surface porosity was still observed. Also, since the weld path involves some overlap of the start and stop points, along a corner, a small region of the weld joint had higher heat input than the rest of the weld. This resulted in a slight divot in that region, which did not leak during pressure testing. Although this spot did not leak during pressure testing, it is still a region subject to stress concentration and therefore, in future experiments, the welding engineer suggests that this overlap region be located along one of the flat edges, rather than the corner, to help eliminate the formation of a high stress concentration. Since surface porosity was small, a PWHT was performed on this sample in an argon atmosphere like EBW_Hex6. Upon initial pressure testing of this sample, a surface pore in the weld on one of the sides of the hex can

began to leak. The location of this leak is indicated in figure 6(g) by a blue arrow. The leak began as soon as pressure was added and bubbling became rapid once a pressure of 20 psi was achieved. The only difference between this sample and sample 6 was a hotter weld pass. The surface porosity may have been a function of a machining defect or the weld parameters themselves. The preheat pass parameters were used to run an interpass both after the weld pass and cosmetic pass to help relieve residual stresses.

EBW_Hex8, shown in figure 6(h), used preheat and interpass weld cycles to maintain an even temperature gradient throughout the weld to prevent cracking caused by high stress concentrations during stress relaxation. Two very small porosity surface defects were observed in this sample (smaller defects than any of the previous samples) and surface defects did not appear to penetrate through the thickness of the weld. The preheat pass parameters were used to run an interpass both after the weld pass and cosmetic pass. After PWHT, pressure testing caused the sample to leak from two points in the weld surface: (1) A surface pore and (2) along the weld in a region where the weld bead appeared slightly cold or displayed some sort of temperature gradient; this region fizzled rather than bubbled. The region where fizzling occurred may have been attributed to microcracking. This sample, along with EBW_Hex6, exhibited the least amount of bubbling upon pressure testing.

EBW_Hex9, shown in figure 6(i), was initially planned to repeat parameters from EBW_Hex8 while only increasing the weld pass to 26 mA. An issue with the EBW machine caused the electron beam to shut off when the 26 mA weld pass was attempted. A preheat pass was rerun prior to attempting the weld pass a second time, and the problem persisted. This was attempted another two times at 25 and 24 mA and, in all cases, the electron beam shut off almost immediately after it turned on. It was then decided to run another interpass at the preheat parameters before putting the unwelded sample in an electrode drying oven at 121.1 °C. The sample was stored for 1 week while the EBW machine was fixed and tested on scrap tungsten to ensure that it functioned properly. Then, the weld cycle was attempted again, starting with a preheat pass and continuing directly into the weld pass at 26 mA. The orientation of the hex can was flipped so the region where the weld started was different than it was 1 week earlier. Next, an interpass weld at the preheat parameters was run, followed by a cosmetic pass at 24 mA, another interpass, and a final cosmetic pass at 25 mA. This final cosmetic pass was used because porosity was present after the initial cosmetic pass and it eliminated the porosity. Lastly, another interpass was run to relieve residual stresses and was followed shortly by the PWHT cycle used on the other samples. At some point between the final interpass and the end of the PWHT cycle, two sidewall cracks propagated from the weld. Both of these propagated from a straight portion of the weld and did not originate at any of the corners. Both cracks leaked during pressure testing. This led to the conclusion that the final cosmetic pass increased the heat input enough to cause brittle fracture due to higher residual stress and the brittle nature of tungsten.[3–5] The results of this weld sample are subject to debate because of the 1-week gap in the weld cycle. Table 1 shows a basic form of the weld schedule used for EBW_Hex6 through EBW_Hex9. These weld schedules were subject to any aforementioned changes made during the welding process.

3.1 Metallographic Analysis

Following PWHT, the eight total plate welds were etched and mounted for metallographic analysis and a brief overview of the metallurgical results is shown in figure 7.
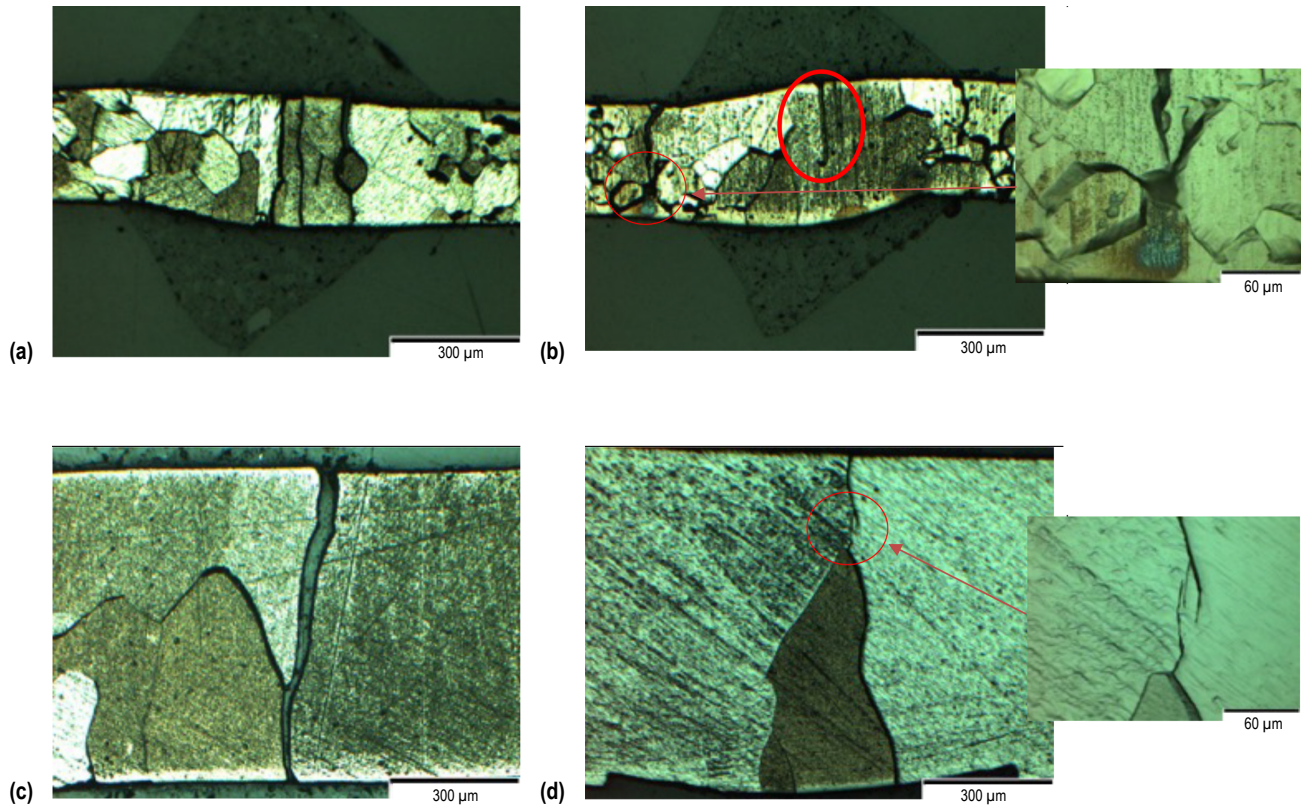

Figure 7. Images of metallography for EBWs joining pure tungsten plate: (a) 0.01-in sample without PWHT showing multiple through-thickness cracks, (b) 0.01-in sample with PWHT showing cracks with increased tortuosity, (c) 0.03-in sample without PWHT showing through-thickness crack, and (d) 0.03-in sample with PWHT showing cracks that did not propagate through-thickness.

Images of metallography from the flat plate samples shown in figure 7 reaffirm that the PWHT helped to reduce through-thickness cracking. The only variation between the samples shown in figure 7(a) and (c) and figure 7(b) and (d) is that the images shown in figure 7(b) and (d) were PWHT at 1037.78 °C within 1 hour after welding commenced. The metallurgical images in figure 7 all show some sort of intergranular cracking and large grain sizes. The samples with no PWHT displayed through-thickness cracks, as shown in figure 7(c) where the crack clearly propagated through the plate and opened up slightly, while the samples with PWHT showed cracks which arrested prior to propagating through the full thickness of the weld. Figure 7(d) displays a 0.03-in sample with a crack that propagated towards an intersection with another crack and, when observed more closely, the crack is not 100% continuous through the thickness of the plate. The 0.01-in samples shown in figure 7(a) and (b) also displayed a variation in the propagation of

cracks through the full thickness of the weld. The image in figure 6(b) shows multiple regions where cracks formed without propagating through the weld completely while the image in figure 6(a) shows multiple through-thickness cracks. This helps indicate that PWHT helped to arrest cracks and prevented through-thickness cracking.

The images shown in figure 8 were taken from the most defect-free regions of EBW_Hex7 and EBW_Hex8 per a visual inspection. EBW_Hex2 was initially chosen for metallography because it did not go through PWHT. During processing for metallography, sample EBW_Hex2 cracked to such a great extent that optical images of the weld were not possible (grains also exfoliated during polishing). EBW_Hex7 and EBW_Hex8 were chosen for metallography because, of the nine hex cans, they exhibited the fewest defects per visual inspection.
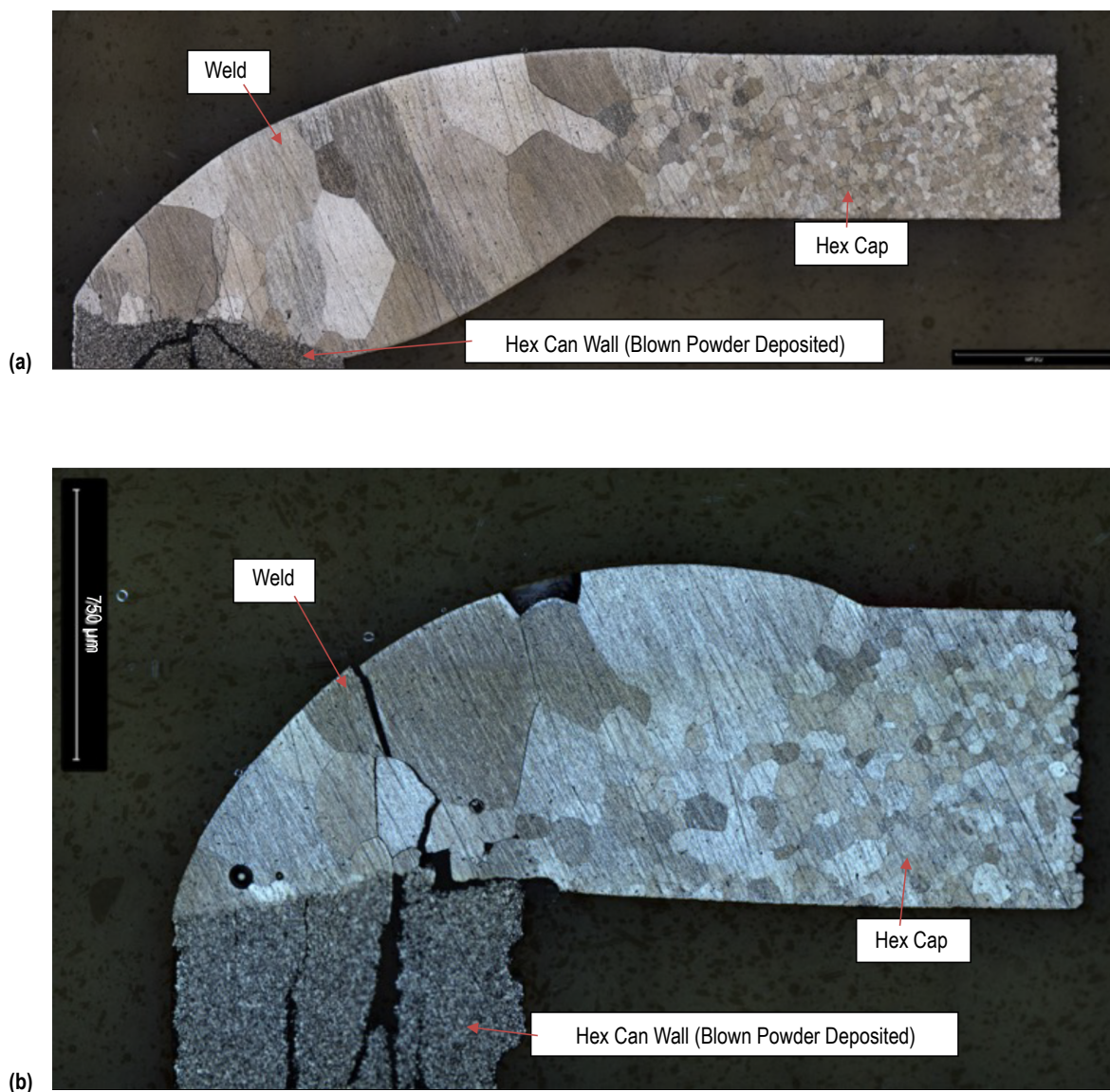

Figure 8. Optical metallography of (a) EBW_Hex7 and (b) EBW_Hex8.

EBW_Hex7 used a slightly lower heat input than EBW_Hex8 for both the weld pass and cosmetic pass. This may have helped refine the grain size slightly, thus increasing resistance to crack propagation from cracks that initiated in the weld heat-affected zone (HAZ) in the hex can wall. The grains in the weld in EBW_Hex8, shown in figure 8(b), are larger on average than the grains in EBW_Hex7, shown in figure 8(a), and therefore the crack propagation path was less tortuous for EBW_Hex8. A straighter crack propagation path for EBW_Hex8 made it easier for cracks to grow through the thickness of the weld, thus creating a leak path. For future experiments on EBW of pure tungsten, a higher number of low heat input passes may be the better approach to prevent cracking due to reduced time for grain growth during the cooling cycle.[9,10]

All of the cracking in the images shown above appear to have initiated in the weld or the HAZ in the hex can wall rather than the hex cap. These two parts of the welded assembly were manufactured with different methods, which may correlate with the occurrence of cracking. The hex can was made with a blown powder deposition process and the hex cap was machined from a plate of pure tungsten. The grain structure varies between these two areas and the HAZ located within the hex cap appears solid and crack free in both of the images shown in figure 8. No cracking or leaking was observed in or from the hex cap in any of the nine samples. The HAZ located within the hex can wall has no apparent grain structure, and crack propagation in this region occurred with little difficulty. The large grains in the weld also formed an easy crack path for cracks that initiated within the hex wall HAZ.[9] As stated before, the weld from EBW_Hex2 was degraded to such a high degree that it fractured multiple times during wire EDM and an optical image of the weld was, therefore, not possible. The extent at which this weld cracked and shattered during cutting and metallography proves that, without a PWHT, welding EBW of pure tungsten would result in a highly brittle and essentially unusable weld. The remaining samples were not analyzed with optical metallography because of a funding constraint and the work associated with processing pure tungsten.

Table 1. Example weld schedules used for EBW_Hex6 through EBW_Hex9.

	Thickness (in)	Preheat FC (MA)	Preheat/ interpass Beam Current (mA)	Preheat Travel Speed (IPM)	Preheat FC (mA)	Preheat Beam Current (mA)	Preheat Travel Speed (IPM)	Weld FC (mA)	Weld Beam Current (mA)	Weld Travel Speed (IPM)	Cosmetic FC (mA)	Cosmetic Beam Current (mA)	Cosmetic Travel Speed (IPM)
W_HEX_EBW6	0.03	540	5.5	4	555	20	4	555	24	4	555	23	4
W_HEX_EBW7	0.03	540	5.5	4	555	20	4	555	26	4	555	23	4
W_HEX_EBW8	0.03	540	5.5	4	555	21	4	555	25	4	555	24	4
W_HEX_EBW9	0.03	540	5.5	4	555	21	4	555	26	4	555	24	4

4. DISCUSSION

Two major factors affect the ability to produce a sound weld in the tungsten hex cans used in this study.:

(1) Geometry of the weld path. The weld follows a hexagonal path so the electron beam must travel around six corners with angles of 120°. Each of these corners can both act as a stress concentration point and a point of high heat input. As the electron beam goes around a corner, the beam location varies from one side of the weld joint to the other, thus causing a temperature gradient to form. To reduce the effect of this, the welder manually controls the location of the electron beam and works to maintain consistency in the weld path. As the experiment progressed, it was clear that a single-point electron beam would cause too great a temperature gradient, leading to hot defects like cracking, or cold defects like porosity. One attempt to mitigate this, as stated earlier, was done by changing the beam pattern so the beam would rotate in a circle rapidly rather than focus on one point to distribute the thermal input more evenly. Another issue with the hexagonal weld path was that the weld speed was difficult to maintain while traveling around the corners. For this reason, the weld schedule developed from the initial plate welds had too high of a travel speed so a new weld schedule with lower travel speed needed to be produced for the hex cans.

(2) Constricted window of acceptable heat input. At a heat input that is too low, the weld either does not fully melt the joint interface or it melts the interface but leaves behind surface porosity. At a heat input that is too high, the weld tends to crack because of embrittlement coupled with high residual stresses focusing on areas of stress concentration. This window of acceptable heat input is yet to be determined because all nine of the hex cans welded resulted in suboptimal welds.

While these two factors made it difficult to produce a leak-tight weld, the visual weld quality clearly improved from EBW_Hex1 to EBW_Hex9. This is evident in figure 6 because EBW_Hex1–5 all had multiple surface defects that were large and EBW_Hex1, 2, and 5 all had through-thickness porosity easily observed in figure 6. EBW_Hex6–9 also had visual defects but they were small and it was not obvious that they penetrated through the thickness of the welds.

High residual stresses have been associated with the impairment of weld ductility.[3] The concentration of heat along a narrow weld path in EBWs helps to reduce the size of the HAZ but also causes high hardness in the HAZ and a high temperature gradient along the edge of the weld.[9] This high temperature gradient can cause residual stresses to build up throughout the weld sample, concentrating on the edge of the weld. Since tungsten is highly brittle,[3–5] it is subject to brittle fracture when stress concentrations are present. A PWHT was added to the experiment for the majority of the welds, both the plate welds and hex cans, and resulted in a decrease in visually observable cracks which propagate from the weld. This was clearly observed in the plate welds shown in figure 5. According to previous research on welding pure tungsten, a PWHT was found to have little effect on the properties of a weld.[7] This is true with regards to metallurgical effects on the tungsten, but a PWHT can be used to relax residual stresses built up during the welding process.[8]

Considering the results of the low-temperature PWHT on the pure tungsten plate welds, a PWHT was added to the hex can weld experiment. The PWHT for the hex cans used a furnace with a greater heating capability and control than the furnace used for the PWHT of the plate welds. This furnace heated the samples to 1400 °C because that temperature was indicated as optimal by a previous research study on pure tungsten EBW.[7] EBW_Hex2 was not PWHT, and days after welding, the hole present in this weld had multiple cracks propagating from it and other cracks propagated from other portions of the weld where microporosity was present. The extent of visually observable cracking increased when observed days after welding with respect to the visually observable cracking found immediately after welding. This may have been due to microcracks that existed immediately after welding and propagated over time as the residual stresses relaxed or new cracks may have formed due to a hydrogen cracking mechanism. Since the welds were made via EBW in a vacuum environment, the likelihood of a hydrogen cracking mechanism is low. The results of visual inspection indicate that cracking was far greater in EBW_Hex2 than EBW_Hex7 and EBW_Hex8 and this was likely due to the lack of PWHT for EBW_Hex2. The likely cause for delayed crack propagation in EBW_Hex2 was residual stress buildup during the weld combined with a high DBTT and the formation of microcracks during the welding process. For EBW_Hex7 and EBW_Hex8, PWHT helped to relax residual stresses evenly, thus arresting the propagation of microcracks.

Immediately after welding, EBW_Hex1 had multiple large holes present like EBW_Hex2, and weeks after welding and PWHT, none of these holes initiated a single crack. The only obvious explanation for the difference in the presence of cracking was that EBW_Hex1 had a PWHT cycle which helped to relieve residual stresses and stress concentrations at the holes.

Previous research also found that a hot preheat weld pass was beneficial in decreasing twinning of the weld and increasing the ductility of an EBW made on pure tungsten. Preventing twinning has also been found to increase ductility and weldability in tungsten welds.[3] A hot preheat pass was not added until EBW_Hex6 after the first five hex cans did not produce satisfactory results. This, along with additional changes to the weld process stated earlier, helped to reduce residual and thermal stresses alongside the weld. Reduced residual and thermal stresses helps to reduce tensile restraint, thus decreasing the likelihood of cracking due to brittle fracture. The changes to the weld schedule improved the visual appearance of the last four hex cans compared to the first five hex cans. EBW_Hex6 also had greatly reduced leaking compared to EBW_Hex1–5 according to a visual observation made during pressure testing. Therefore, both the visual appearance and the performance during pressure testing improved when a hot preheat pass and a rotating beam pattern were incorporated into the weld schedule.

Drastic improvement in visual appearance and reduced leaking during pressure testing indicates that hex can welds improved from EBW_Hex1 to EBW_Hex9. Although the welds improved from EBW_Hex1 to EBW_Hex9, and EBW_Hex6 to EBW_Hex8 produced the best results, none of the welds held pressure consistently and all of them, except EBW_Hex9, had visual porosity. EBW_Hex9 was only porosity free because weld passes were repeated until the visual porosity was consumed by the weld bead. This led to higher heat input which caused the sample to crack in the weld and along the side wall of the hex can.

As shown in the metallography images in figure 8, all cracks that formed were found on the side of the weld closer to the hex wall or within the HAZ located in the hex wall. This could be attributed to the grain structure and material properties of the hex wall and/or the increased stress concentration found on the radius of the weld. Since the cracks all formed in the hex wall rather than the hex cap, the blown powder deposition process used for the hex wall is not a satisfactory process for forming tungsten. The grain structures attained from a rolled tungsten plate has been successful in resisting crack growth because no crack formed in the hex cap in any of the nine hex cans.

5. CONCLUSION

This experiment was done to assess the ability to manufacture a pure tungsten hex can for NTP applications. The results of part 1 of the experiment proved that a PWHT was beneficial in preventing or arresting cracks that propagate from tungsten EBWs.

Both parts 1 and 2 of the experiment were met with barriers but determined ways to improve the appearance and performance of a pure tungsten EBW. Weld properties improved from EBW_Hex1 to EBW_Hex9 but none of them held pressure. At low heat input, the hex can welds tended to form porosity, and at high heat input, they tended to crack. This cracking may have been linked to brittle overload fracture due to high residual stresses and a very high DBTT.[3–5] The result of this experiment was the knowledge that a preheat, PWHT, multiple weld passes with low heat input, and a rotating beam pattern all increase the quality of a pure tungsten EBW based on visual appearance and the number and size of cracks. It also resulted in the knowledge that, in comparison to pure tungsten parts manufactured with blown powder deposition, pure tungsten rolled plate has a strong resistance to cracking during EBW. The additions to the weld cycle discovered in this experiment also appear to increase the likelihood of generating a pure tungsten weld capable of a hermetic seal. Overall, this experiment has yielded the knowledge that electron beam welding of pure tungsten has difficulties but, with additional research and development, has great potential for success.

6. RECOMMENDATIONS

All additional experiments shall take the key points from this experiment, such as adding a PWHT, a hot preheat pass, and using a rotating beam pattern, and shall work to determine the heat input range over which samples are free of porosity and cracking. An EBW machine with furnace capability may be used to preheat the entire tungsten weld sample instead of a preheat weld pass. This would help to ensure an even temperature preheat, therefore, preventing the buildup of residual stresses caused by high temperature gradients. To decrease the likelihood of cracking in pure tungsten EBWs, it is important to use tungsten with a grain structure similar to the structure shown in the hex caps in the metallography images in figure 8. Future experiments may also use tungsten alloyed with a low percentage of rhenium because rhenium has been found to increase the ductility of tungsten.[4,11]

Figures in the appendix show the weld fixture (fig. 9), the EBW machine (fig. 10), the EBW machine operators interface (fig. 11), the pressure hose and aluminum hex fitting (fig. 12), the tube furnace (fig. 13), extent of cracking in the hex can side wall (fig. 14), schematic of hex can/pressure fitting (fig. 15), and the type of heat gun used (fig. 16).

Figure 9. Weld fixture (with EBW_Hex6 in place prior to welding).

Figure 10. EBW machine used to weld both pure tungsten plates and pure tungsten hex cans.

Figure 11. EBW machine operators interface.

Figure 12. Pressure hose and aluminum hex fitting designed to pressurize the EBW tungsten weld. Polymer binder applied using a heat gun to make the interface leak tight.
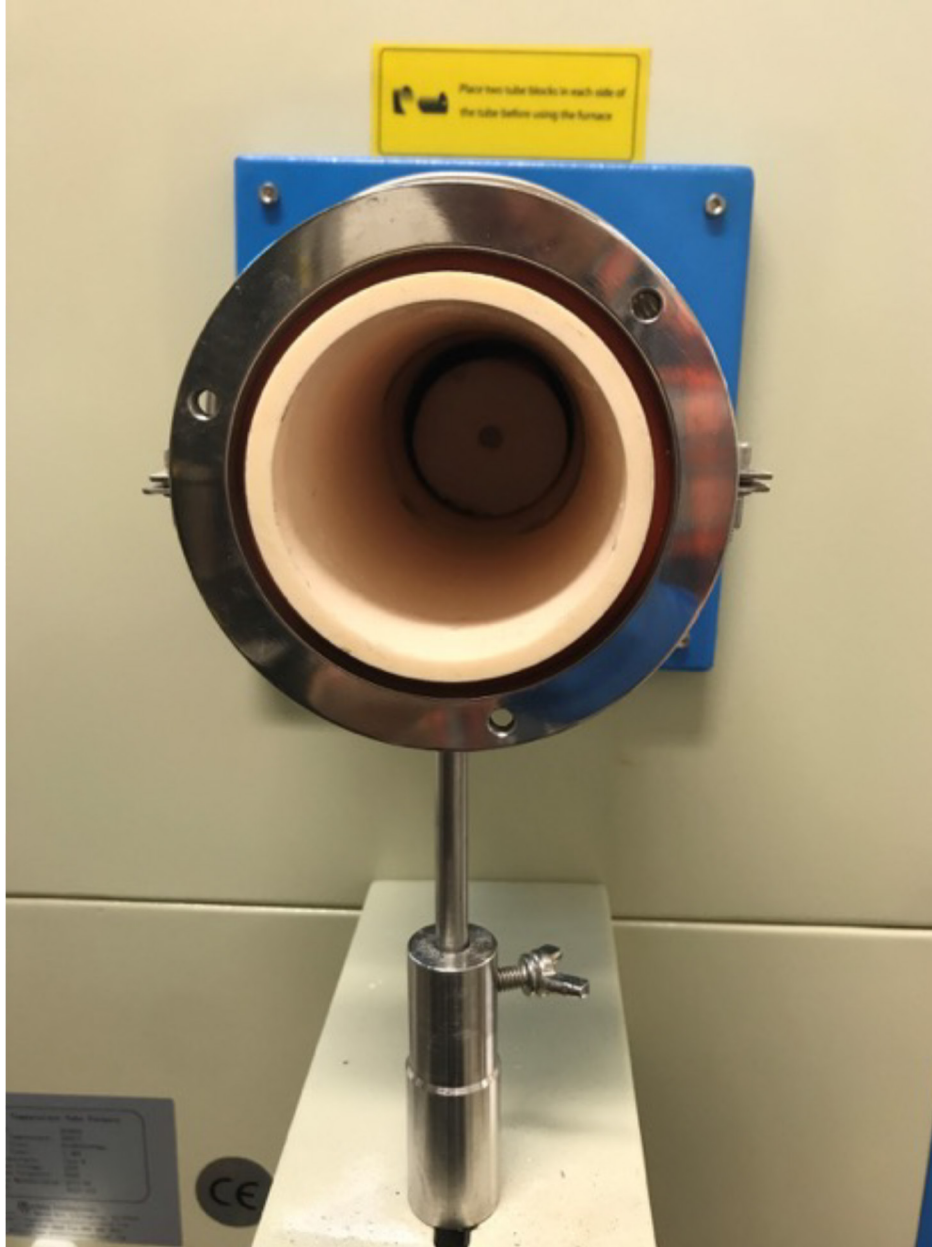
Figure 13. Tube furnace used to PWHT tungsten hex cans.

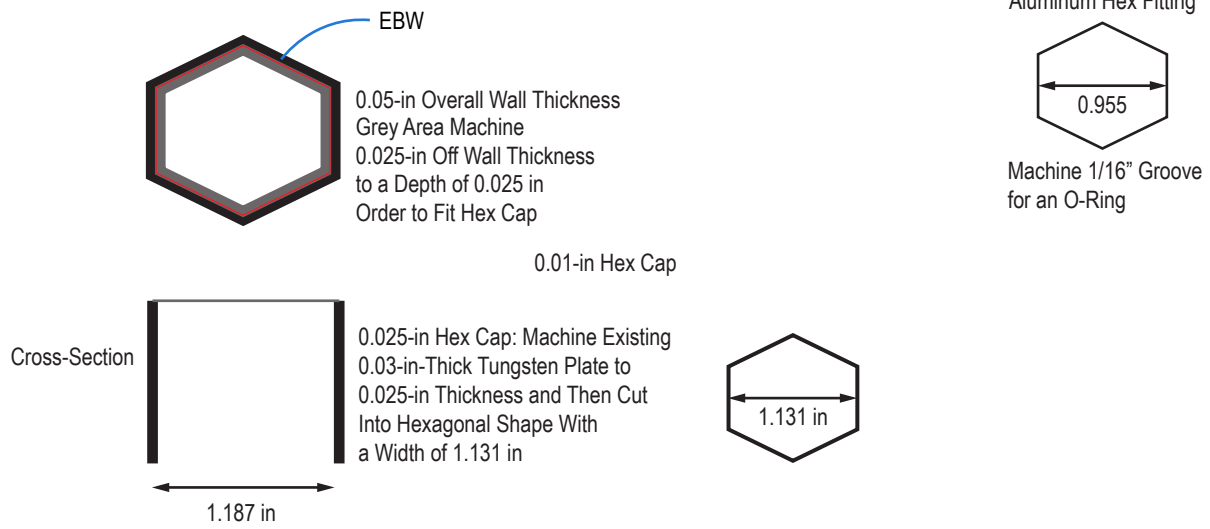Figure 14. EBW_Hex8 unetched showing the extent of cracking in the hex can side wall.

EBW

0.05-in Overall Wall Thickness
Grey Area Machine
0.025-in Off Wall Thickness
to a Depth of 0.025 in
Order to Fit Hex Cap

Aluminum Hex Fitting

0.955

Machine 1/16" Groove
for an O-Ring

0.01-in Hex Cap

Cross-Section

0.025-in Hex Cap: Machine Existing
0.03-in-Thick Tungsten Plate to
0.025-in Thickness and Then Cut
Into Hexagonal Shape With
a Width of 1.131 in

1.131 in

1.187 in

Figure 15. Basic hex can and pressure fitting design schematic.

Figure 16. Heat gun used to heat polymer for pressure testing.

REFERENCES

1. Finseth, J.L.: "Rover Nuclear Rocket Engine Program," NASA-CR-184270, NASA Marshall Space Flight Center, Huntsville, AL, February 1991.

2. Webster, J.R.P.: "Introduction to Neutron Reflectivity," ISIS Neutron Scattering Training Course: Large Scale Structures Module. Science & Technology Facilities Council, ISIS Facility, Rutherford Appleton Library, 2010.

3. "Development of Ductile, Bulk Tungsten for Next Generation Munitions and Warheads," Department of Defense, 2013.

4. Raffo, P.L.: "Yielding and fracture in tungsten and tungsten-rhenium alloys," *Journal of the Less Common Metals*, Vol. 17, Issue 2, pp. 133–149, February 1969.

5. Lassner, E.; and Wolf-Dieter, S.: "Tungsten—Properties, Chemistry, Technology of the Element, Alloys and Chemical Compounds," Vienna University of Technology, 1999.

6. "More Tungsten information," <https://www.tungsten.com/more-tungsten-information/>, Midwest Tungsten Service.

7. Lessmann, G.G.: "Determination of weldability and elevated temperature stability of refractory metal alloys. 1—Weldability of refractory metal alloys," National Aeronautics and Space Administration, September 1970.

8. Khaled, T.: "Preheating, Interpass and Post-Weld Heat Treatment Requirements for Welding Low Alloy Steels," Federal Aviation Administration, ANM-112N-14-02, Rev. A, October 22, 2014.

9. Schubert, G.: "Electron Beam Welding Process, Applications and Equipment," PTR, Precision Technologies, Inc., 7 pp.

10. Herring, D.H.: "Grain Size and its Influence on Material Properties," Industrial Heating's The Heat Treat Doctor, August 2005.

11. "Rhenium and Alloys," <http://what-when-how.com/materialsparts-and-finishes/rhenium-and-alloys/>, What-When-How In Depth Tutorials and Information.

1. REPORT DATE *(DD-MM-YYYY)* 01–06–2019	2. REPORT TYPE Technical Memorandum	3. DATES COVERED *(From - To)*

4. TITLE AND SUBTITLE Electron Beam Welding of Pure Tungsten Hex Cans for Nuclear Thermal Propulsion Engines	5a. CONTRACT NUMBER
	5b. GRANT NUMBER
	5c. PROGRAM ELEMENT NUMBER

6. AUTHOR(S) Z.S. Courtright and K.M Benensky	5d. PROJECT NUMBER
	5e. TASK NUMBER
	5f. WORK UNIT NUMBER

7. PERFORMING ORGANIZATION NAME(S) AND ADDRESS(ES) George C. Marshall Space Flight Center Huntsville, AL 35812	8. PERFORMING ORGANIZATION REPORT NUMBER M–1486

9. SPONSORING/MONITORING AGENCY NAME(S) AND ADDRESS(ES) National Aeronautics and Space Administration Washington, DC 20546–0001	10. SPONSORING/MONITOR'S ACRONYM(S) NASA
	11. SPONSORING/MONITORING REPORT NUMBER NASA/TM—2019–220135

12. DISTRIBUTION/AVAILABILITY STATEMENT
Unclassified-Unlimited
Subject Category 26
Availability: NASA STI Information Desk (757–864–9658)

13. SUPPLEMENTARY NOTES
Prepared by the Materials & Processes Laboratory, Engineering Directorate

14. ABSTRACT

A preliminary investigation was undertaken to determine whether electron beam welding can produce airtight welds to seal pure tungsten hex cans developed for fuel system cladding nuclear thermal propulsion applications. Initial studies on welds in 0.01- and 0.03-in-thick tungsten exhibited cracks. The occurrence of the cracks was reduced but not eliminated by a post-weld heat treatment at 1038 °C. Cracking was less severe in thicker metal and did not always penetrate the entire thickness. The investigation was continued welding 0.025-in-thick hexagonal caps onto 0.05-in-thick cans. Sound appearing welds were pressure tested under water for leakage at up to 20 psi. Although sound appearing welds were achieved, all of the nine cans available for testing leaked under pressure testing. The leakage was associated with the cans, produced by blown powder deposition, and not with the wrought metal caps.

15. SUBJECT TERMS
electron beam weld, tungsten, nuclear propulsion

16. SECURITY CLASSIFICATION OF:			17. LIMITATION OF ABSTRACT	18. NUMBER OF PAGES	19a. NAME OF RESPONSIBLE PERSON STI Help Desk at email: help@sti.nasa.gov
a. REPORT	b. ABSTRACT	c. THIS PAGE	UU	40	
U	U	U			19b. TELEPHONE NUMBER *(Include area code)* STI Help Desk at: 757–864–9658

National Aeronautics and
Space Administration
IS02
George C. Marshall Space Flight Center
Huntsville, Alabama 35812